Au cluster formation on a pore containing membrane under the various surface treatments

Seong Soo Choi, Sae-Joong Oh, Chul Hee Han, Doo Jae Park, Soo Bong Choi, Yong-Sang Kim, and Nam Kyou Park

Citation: Journal of Vacuum Science & Technology B, Nanotechnology and Microelectronics: Materials, Processing, Measurement, and Phenomena **35**, 04F107 (2017); doi: 10.1116/1.4994828

View online: http://dx.doi.org/10.1116/1.4994828

View Table of Contents: http://avs.scitation.org/toc/jvb/35/4

Published by the American Vacuum Society

Au cluster formation on a pore containing membrane under the various surface treatments

Seong Soo Choi[a)]
Research Center for Nanobio Science, SunMoon University, Ahsan, Chungnam 31460, South Korea

Sae-Joong Oh and Chul Hee Han
Research Center for Nanobio Science, SunMoon University, Ahsan, Chungnam 31460, South Korea

Doo Jae Park
Department of Physics, Hallym University, Chuncheon 24252, South Korea

Soo Bong Choi
Department of Physics, Inchon National University, Inchon 22012, South Korea

Yong-Sang Kim
School of Electronic and Electrical Engineering, Sungkyunkwan University, Suwon, Gyeong-Gi-Do 16419, South Korea

Nam Kyou Park
School of Electrical Engineering, Seoul National University, Seoul 08826, South Korea

(Received 14 March 2017; accepted 7 July 2017; published 26 July 2017)

In this report, the authors will investigate the formation of Au clusters on the nanoscale membrane formed during various surface treatments such as electron beam irradiations, Ga ion focused ion beam (FIB) technique, and thermal treatment. Nanoapertures on the freestanding Au film were fabricated by using FIB technique, and a nanometer scale membrane created in the aperture by various surface treatments. Transmission electron microscopy reveals that Au clusters has formed on the membrane after the sample storage at room temperature for several months. In addition, Au clusters on the carbon-containing membrane were also observed after surface treatments of Ga ion beam etching, and thermal heating of freestanding 40 nm thick Au film at temperatures ranging from 400 to 800 °C. Spinodal decomposition, spinodal dewetting, and coalescence of the Au particles on the carbon-containing membrane were also observed. © *2017 American Vacuum Society*. [http://dx.doi.org/10.1116/1.4994828]

I. INTRODUCTION

There have been many reports about fabrication of the solid state nanopore by using ion sculpting technique and high energy electron beam techniques such as field emission scanning microscopy (FESEM) and transmission electron microscopy (TEM) due to the capabilities of single molecule nanobio sensor.[1–5] A nanopore device with an electrical detection technique has been successfully fabricated by Oxford Nanopore Technology. However, this portable nanopore device is reported to present relatively high error rates, even though significant improvements have been made.[6–8] Current genome sequencing technique and many other nanobio sensor devices are based on the optical detection methods. However, the optical nanopore device has not been developed yet.

We reported previously the fabrication of nanopore on the electron beam induced Au-C binary mixture membrane.[9–12] We reported that diffusion of Au and C under the electron beam irradiations would occur and forms the binary mixture membrane with Au and C atoms. Furthermore, when the samples irradiated by the electron beam were stored for one year in a room environment, Au clusters on the diffused membrane were growing via Ostwald ripening.

The early stages of vacuum-deposited Au film is reported to consist of Au particles and clusters with various sizes and shapes such as multiple twin particles (MTP) with a decahedron shape and an icosahedron shape.[13–15] Melting temperature of Au nanoparticle is lower than that of Au bulk, down to a few hundred Celsius for ~5 nm diameter Au particle. The main physical reason is that smaller particles have larger surface to volume ratio, and the surface atoms have lower binding energy. The melting temperature of Au clusters is also dependent upon the size, geometrical shape, and numbers of Au atoms in the cluster through so-called magic numbers.[16–19]

When electron beam irradiation is performed by using FESEM, the pore size always shrinks, regardless of the ratio of the specimen thickness to the aperture diameter.[3–5] For 2 keV accelerating energy of FESEM, most of electron energy will be deposited into the surface layer with a thickness less than 100 nm.[20] Hence, an electron beam irradiation at 2 keV on the sample surface would provide the surface diffusion for nanopore formation on the specimen from electron beam induced melting and local temperature rise.[16,17,21,22]

On the other hand, for high energy TEM electron beam irradiations on the aperture, its size will either shrink or become open, depending upon the ratio of specimen

[a)]Also at School of Electronic and Electrical Engineering, Sungkyunkwan University, Suwon, Kyung Gi Do 16419, South Korea; electronic addresses: sscphy2010@ gmail.com; 1982@daum.net

thickness to the aperture diameter.[1,2,23,24] Resizing the aperture on the viscous specimen surface is well documented before.[1–5] This phenomenon has been described by the surface tension on the viscous specimen surface under electron beam irradiations. Depending upon temperature and viscosity of the heated membrane, the surface tension force, and the vapor pressure of the material, pore widening and shrinking are expected to occur. During high energy TEM electron beam irradiations at ~200 kV, most of the electrons would be transmitted, However, due to the inelastic collisions such as Coulomb explosion of electrons, electron beam induced thermal spike,[25–30] nanoscale local temperature rise followed by melting, sputtering and evaporation have also been reported.[30–33] Nanoscale Au particles have lower displacement energy and threshold energy than those of Au bulk. Therefore, under a 200 keV electron beam irradiation, knock-on and displacement of Au nanoparticles could occur.

Under electron beam irradiations on the focused ion beam (FIB) drilled Au aperture on the specimen, the Au and C atoms would diffuse into the aperture and form the nanometer thick Au membrane incorporated with carbon atoms. Carbon encapsulation of Au atoms under heating and Au evaporation during TEM imaging have also reported in the literature.[34,35] It has been reported that Au atoms become more stable with carbon atoms than without carbon atoms.[36,37] Au cluster formation and island formation on the amorphous carbon film has also been reported after the sample was stored under room temperature for a few months or more.[10,32] However, when Au atoms smaller than 1 nm are deposited on the amorphous carbon, imaging of Au atoms was not possible due to low contrast on the amorphous substrate by TEM. During a sample storage period for several months under a room environment, small Au particles condense into larger particles. This phenomenon is attributed to Ostwald ripening process; large particles are thermodynamically more favorable than small particles.[38–40] All the small particles will shrink, and the larger particles will grow and become bigger.

Several of the phenomena and processes under high energy electron beam irradiation of a binary system has been modeled in a wider perspective for thermodynamic unstable systems, for example, spinodal decomposition,[41] cluster formation,[42] and Ostwald ripening.[43] Under thermal treatment of the metallic film, spinodal dewetting of the liquid metallic film was reported, along with hole nucleation and growth.[44,45]

In this report, we investigate the Au cluster formation phenomenon on the nanoscale membrane formed under various surface treatments, including electron beam irradiation, FIB etching, and thermal treatment.

II. EXPERIMENTAL PROCEDURES AND RESULTS

A. Sample preparation

TEM grid samples with (100 × 100 μm) SiN or SiO_2 membranes were initially purchased from TEMwindows Company (www.temwindows.com). Then, Au thin films were deposited by using physical vapor deposition technique. We used Au film thickness of 200 nm for the experiments reported in Sec. II B–II F and 40 nm for that in Sec. II G. The deposition was followed by dry plasma etching of the supporting layer of SiN or SiO_2. This backside etching process would make a freestanding Au film in a (100 × 100 μm) size window. Then, the Au apertures on the freestanding Au film were drilled by using a 30 keV FIB (Dual beam Helio, FEI) technique, followed by various electron beam irradiations. We used various TEM and FESEM apparatuses for the irradiations as a means to vary the electron energy. We used two TEM (JEM-2100F, and JEM-3100HR) and FESEM (JSM 6400) from the National Nanofabrication Center, Daejeon, South Korea, to observe the results of the irradiations. We generally used similar settings for irradiations and for imaging.

B. Membrane formation by TEM high energy electron beam irradiations

An array of Au aperture on a 200 nm thick Au film was drilled by 30 keV FIB (Dual beam Helio, FEI); then, various electron beam irradiations were carried out to form the membrane inside the FIB drilled aperture. Electron beam irradiations were performed at 300 keV for the experiments described in this section.

When a high energy electron beam was irradiated on the Au film, the irradiated specimen area become viscous, the Au atoms along with C atoms (from hydrocarbons in the vacuum) would diffuse and form an Au-C binary membrane, when the aperture diameter becomes smaller than the film thickness. A (5 × 5) aperture array on a 200 nm thick Au film is presented in Fig. 1. The fabricated diameter and the pitch of the aperture array is ~120 nm diameter and 0.49 μm, respectively.

Figure 2 presents the TEM images of the Au apertures before and after electron beam irradiations. Electron beam irradiations were carried out on the center aperture B2 (inside the yellow circle). The apertures have been labeled according to row and column in Fig. 1. Figures 2(a) and 2(b) show the aperture B2 before and after electron beam irradiation. The white oval (120 × 150 nm) area in the images are the opening of the aperture. The gray area surrounding

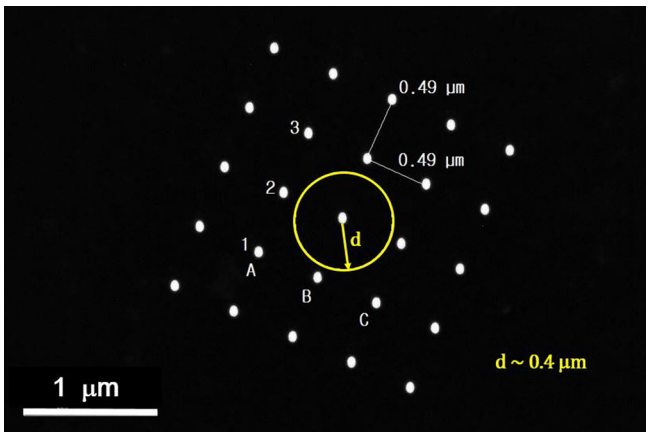

FIG. 1. (Color online) TEM image of the aperture array on the 200 nm Au free standing film is shown. The aperture array with its diameters of ~120 nm was drilled by using 30 keV Ga ion keV. The pitch was measured to be 0.49 μm. The fabricated aperture array was tested to measure the thermal influence on the aperture during 300 keV electron beam irradiations. The electron beam was irradiated on the area inside the yellow circle with a 0.4 μm diameter.

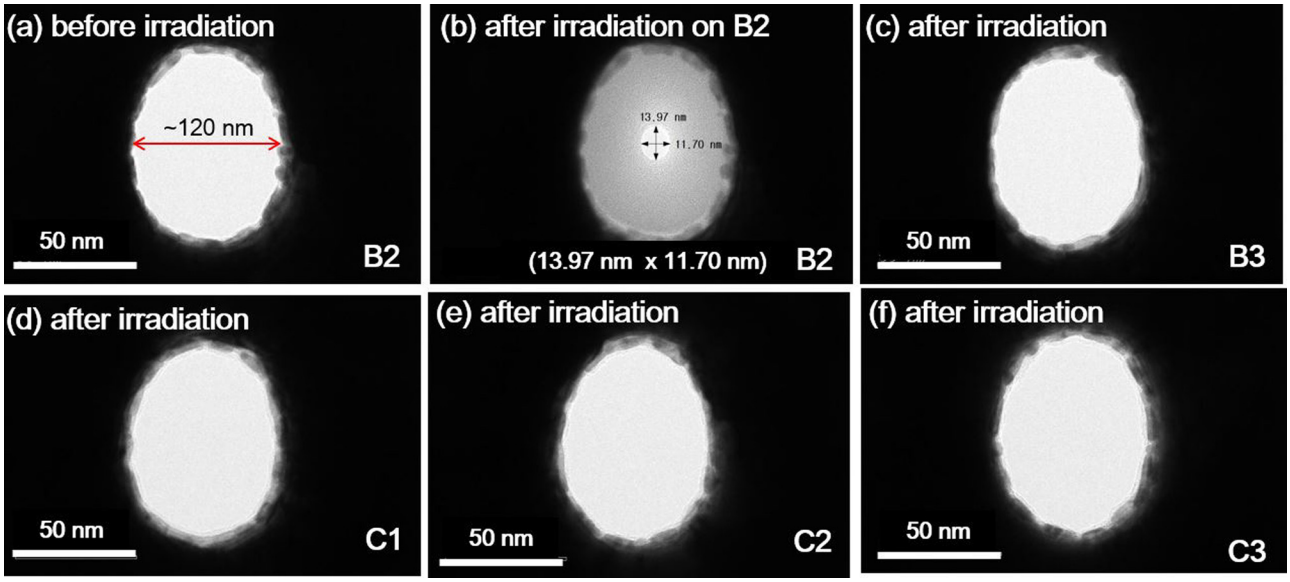

FIG. 2. (Color online) TEM images of the apertures in the 200 nm thick self-supporting Au film before and after electron beam irradiation. Only the B2 aperture was irradiated. Other apertures close to the center aperture B2 are labeled as B3, C1, C2, and C3. A TEM image of the FIB drilled Au aperture B2 with its size of (120 × 150 nm) on a 200 nm Au film is shown before the electron beam irradiation in (a). After a 2 pA electron beam irradiation at 300 keV for 10 min on the B2 aperture, a (13.97 × 11.70 nm) size pore was formed (b). However, no other apertures presented the formation of membranes except the B2 aperture.

the oval area is the beginning of membrane formation. In Fig. 2(a), a membrane has been formed on the periphery of the aperture during the FIB drilling opening the aperture. The large increase in the gray area shown in Fig. 2(b) compared to that of Fig. 2(a) is due to the growth of the membrane during the electron irradiation. The electron irradiation for the experiments described in Fig. 2 were done *in situ* in the TEM with a 2 pA beam for 5 min at 300 keV. The projection type beam was maintained over the area indicated by the yellow circle (0.4 μm diameter) in Fig. 1. However, no pore membranes were formed from any adjacent apertures, other than B2 aperture. These particular experimental result indicates that the thermal influenced area is limited to an electron irradiated area, and it may be attributed to the electron beam induced thermal spike.[24–28]

We also investigated membrane formation which is dependent upon the electron beam current under high energy electron beam irradiations at 300 keV. Figure 3 presents the TEM images of the FIB drilled apertures depending upon the electron beam current densities of 5 and 10 pA/cm^2. A TEM image of the drilled Au aperture is shown in Fig. 3(a). The diffused

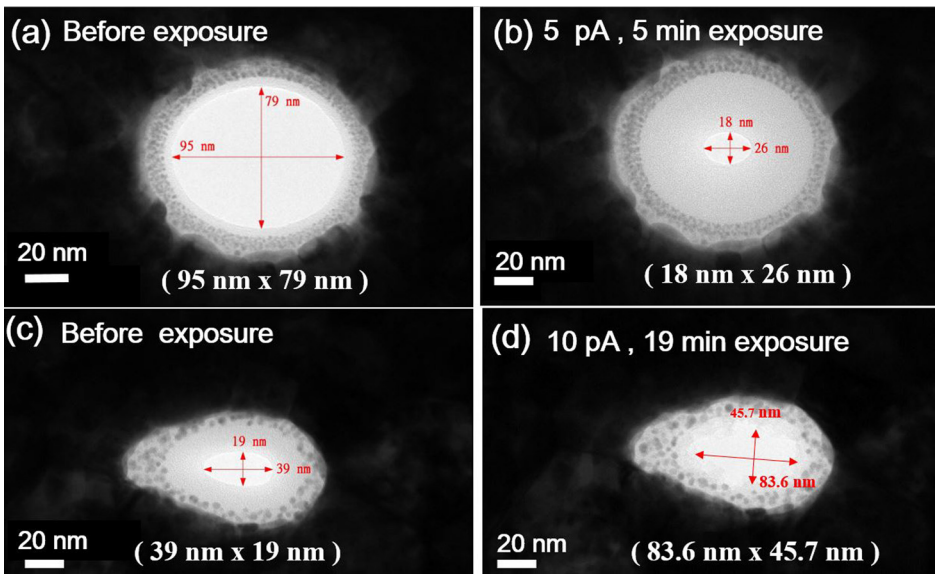

FIG. 3. (Color online) TEM images of the FIB drilled apertures dependent upon the electron beam irradiation conditions. The (95 × 79 nm) size Au aperture was initially drilled by using 30 keV FIB technique in (a). The gray area on the periphery of the aperture indicates the diffused area due to Ga ion induced thermal spike during FIB milling. Au clusters formed during FIB drilling are shown around the periphery of the drilled aperture. Under 5 pA electron beam irradiations, the (18 × 26 nm) size pore was formed in (b). However, under 10 pA electron beam irradiations, the (19 × 39 nm) size pore on the diffused membrane in (c) was widened into the (45.7 × 83.6 nm) size aperture in (d).

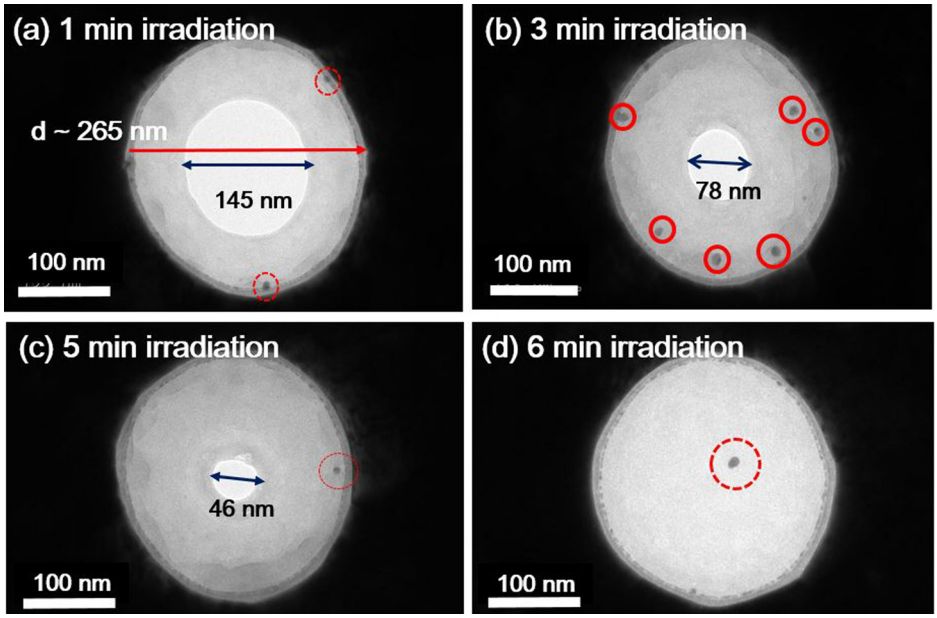

FIG. 4. (Color online) TEM images present the pore membrane formation by using 2 keV FESEM electron beam irradiations, and Au cluster formation on the diffused pore-membrane is presented after the sample was stored under a room environment for five months. The drilled aperture with its diameter of ~265 nm is presented in (a). Initially, pore formation using 2 keV electron beam irradiations for 1, 3, 5, and 6 min was carried out. The corresponding pore diameters are 145 nm (a), 78 nm (b), 45 nm (c), and 0 nm (d). For these particular samples, the shapes of the pore diameters have not been changed after the sample was stored for several months under the room environment. Only Au nanoparticles on the diffused membranes had formed.

gray area with Au clusters on the periphery of the (95×79 nm) aperture is formed due to the thermal spike during FIB drilling.[24] After 300 keV, 5 pA/cm^2 electron beam irradiation, an (18×26 nm) opening on the diffused membrane is formed as shown in Fig. 3(b). However, under 10 pA electron beam irradiation, the (19×39 nm) size opening on the diffused membrane, shown in Fig. 3(c), was widened into the (45.7×83.6 nm) size opening in Fig. 3(d). This may be attributed to sputtering or evaporation of the atomic element on the diffused layer from high energy electron beam irradiation.[31,32]

C. Membrane formation by FESEM electron beam irradiations

We have drilled Au aperture with its diameter greater than the thickness of the Au film. For the aperture diameter greater than the 200 nm Au film thickness, low energy scanning electron beam irradiation using FESEM is required for the fabrication of the membrane. With electron beam irradiation using FESEM, diffusion of atoms will occur and the pore membrane will be formed inside the aperture, regardless of the ratio of aperture diameter to film thickness.

Several Au apertures with ~265 nm diameter were drilled on a ~200 nm Au film by using 30 keV FIB technique, followed by 2 keV, 1.4 nA electron beam irradiations by using FESEM (installed with Dual beam Helio, FEI) for 1, 3, 5, and 6 min periods. For 2 keV FESEM electron beam irradiation, most of electron energy will be deposited into the surface layer of the Au less than ~100 nm.[22] The beam was scanned with the following scanning data: scanning area of ($\sim 1 \times \sim 1$ μm), 300 μs dwell time, and 1.5 nm beam spotsize. We assumed that under the given conditions the surface area will melt, similar to the surface layer of small particles.

Figure 4 shows the TEM images of openings with Au clusters on the pore membranes under the room environments for five months after electron beam irradiation. The diameters of the openings in the pore membrane for 1, 3, 5, and 6 min irradiation are measured to be 145, 78, 45, and 0 nm, respectively. No change in the size or shape of the pore openings were observed even under the room environment for five months. Au clusters had formed and grown under Ostwald ripening in the diffused membrane and are indicated by red circles.

D. Energy dispersive x-ray spectroscopy on the electron beam induced membrane

Chemical analysis for the 2 keV FESEM electron beam induced membrane in an Au aperture was also performed by using energy EDS system with a scanning TEM (STEM, JEOL 2100F). The EDS analysis system by using 200 keV STEM can provide a better qualitative results, rather than EDAX analysis system by using FESEM due to a larger and better detector system at 200 keV STEM. The focused electron beam probe with a 1.5 nm diameter is set to 2.5 nA probe current at 200 keV and 1 min duration time. Two Au clusters formed inside the red circles are shown in Fig. 5(a). The energy dispersive spectroscopy (EDS) line scan profile is also shown in Fig. 5(b), and the average atomic concentrations of Au, C, and O for this particular sample are measured to be ~80%, ~20%, and less than 10%, respectively.

E. Au cluster and lattice structures on the Au-C binary membrane

Figure 6 shows an Au cluster that formed on the diffused membrane in the Au aperture on a 200 nm Au film by a

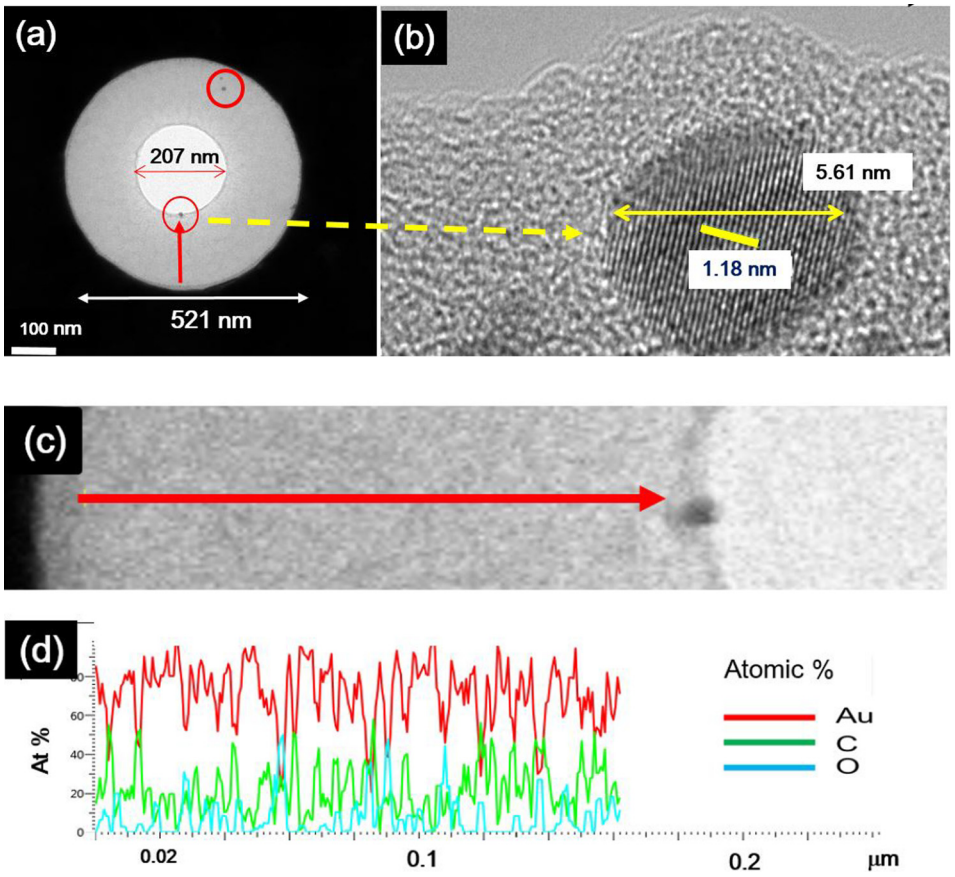

FIG. 5. (Color online) TEM image of a 207 diameter pore on the membrane on the 521 nm diameter Au aperture (a). Two Au clusters formed on the membrane are also shown in (a), and the enlarged image of the Au cluster on the edge of the pore (inside the red circle) is presented as a ~5.61 nm size Au MTP with a ten crystal lattice spacing of 1.18 nm in (b). The red solid arrow (a) presents the line profile of EDS on the diffused membrane in (c). The profiles of the Au, C, and O atomic concentrations on the line are given in (d). On this particular sample, the uneven concentration profiles along the line for Au, C, and O is shown. The corresponding average atomic concentrations for Au, C, and O are approximately ~80%, 20%, and less than ~10%, respectively.

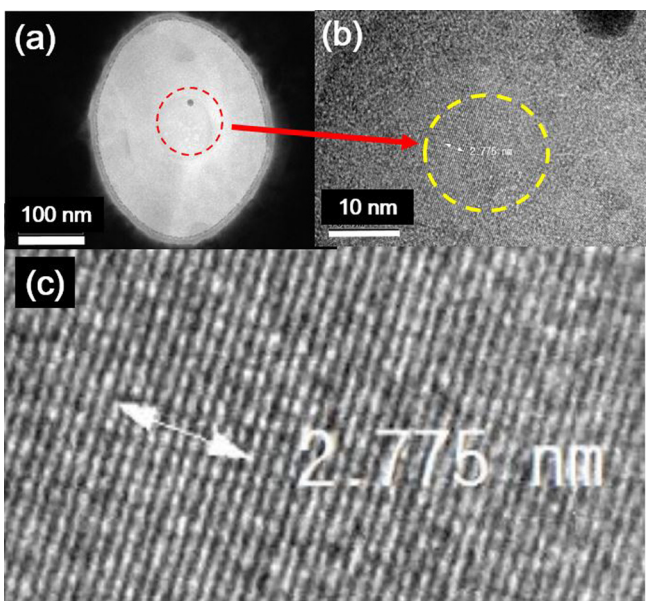

FIG. 6. (Color online) TEM images of Au cluster in (a), and Au lattice formation on the diffused membrane is shown in (b) and (c). The lattice spacing for 10 rows is given as 2.775 nm as in (c). The Au-C binary mixture membrane undergoes from amorphous mixture state of Au and C to the formation of a crystalline structure due to spinodal decomposition under an electron beam irradiation.

300 keV TEM. The magnified TEM images of the enlarged dotted circled area in (a) is provided in Figs. 6(b) and 6(c). The area inside the dotted yellow circle is magnified to exhibit the Au lattice structure of 2.775 nm for ten atomic rows formed on the diffused membrane. Figure 7 presents the formation of the Au crystalline lattice structure on the diffused membrane during a 300 keV electron beam irradiation.

During electron beam irradiation, the images were taken with approximately 2 s interval. The Au lattice structure with a lattice spacing of 2.776 nm for ten rows is shown in Fig. 7(a), and two other areas do not present the lattice structure. The structures were continuously changed under an electron beam irradiation. However, 2 s later, the three areas present the lattice spacing for ten rows: 3.576 nm inside the dotted circle to bottom left, 2.781 nm inside the dashed circle at the center, and 3.939 nm inside the black dashed circle at the top right in (b).

E. Au cluster and membrane formation under FIB Ga ion irradiation treatment.

Figure 8 shows the TEM image of the Au clusters on the thin membrane formed on the etched area by FIB. TEM image of the (~280 × ~200 nm) membrane is presented along with two open pores (A and B) formed after exposure to 1.4 nA,

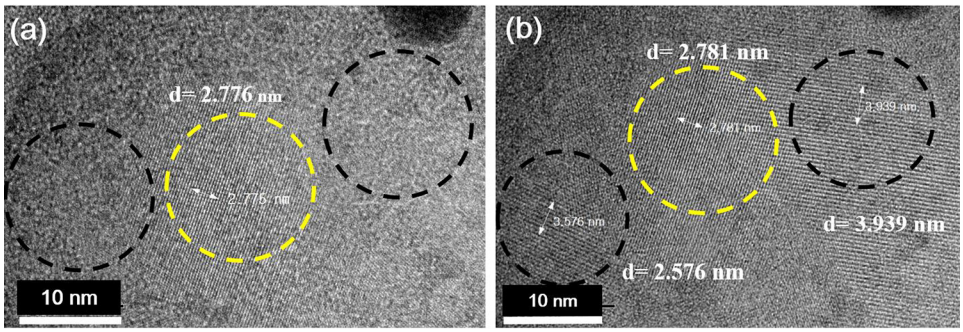

FIG. 7. (Color online) TEM images of spinodal phase change under an electron beam irradiation are presented. Images were taken with ~2 s interval during an electron beam irradiation at 300 keV. An Au crystal lattice with 2.775 nm for ten rows is shown inside a dashed circle at the center in (a). The areas inside both a dashed circle at the bottom left and a black dashed circle at the right top do not show any Au lattice images. However, after 2 s later, Au lattice structures are presented: 2.576 nm for bottom left circle, 2.781 nm for center circle, 3.939 nm for black dashed top right circle.

30 keV Ga ion beam for 1 s on the sample in Fig. 8(a). We also observed that these pores became closed after being kept under room environment for several months. One of the Au cluster with (~19.5 × ~11 nm) is magnified in Fig. 8(b) showing the Au lattice. The Au cluster has also been analyzed using EDS. The average atomic concentration percentages of Au, C, and O on the etched area by EDS analysis is found to be 52,4%, 46.3%, and 1.3%, respectively (supplementary material 1).[46]

G. Thermal treatment on a freestanding 40 nm thick Au film

We carried out thermal treatment on the sputter-deposited 40 nm thick Au film. The sample was inserted in the heating stage of TEM equipment (HR TEM 3100). It took about 30 min to increase the temperature up to 400 °C from room temperature. Figure 9(a) presented a TEM image of the Au film after the temperature was increased up to 400 °C. Upon heating, a hole generation was observed. A 59.6 nm diameter hole surrounded with a diffused membrane is formed. Numerous tiny Au particles are uniformly distributed on the gray diffused membrane. Upon 300 keV electron beam irradiation for 10 min, the tiny Au clusters are coalesced into larger Au clusters via Ostwald ripening. The measured diameter of one Au cluster in Fig. 9(b) is ~5.7 nm (inside the blue circle). The circular opening with a 59.6 nm diameter in Fig. 9(a) got a bigger circular opening with an 84.8 nm diameter in Fig. 9(b). Figure 10 presents the TEM images after thermal treatments at 600 and 800 °C, with and without electron beam irradiations. The formation of the 64.8 nm diameter holes surrounded with Au-C mixture membrane along with several scale thick membranes is presented in Fig. 10(a) for 10 min heating at 600 °C without electron beam irradiation. After increasing the temperature up to 800 °C, no significant change in the hole shape is observed and even at another 10 min heating at 800 °C in Fig. 10(b). However, for a 10 min electron beam irradiation at 800 °C, holes merged and became into a larger hole with a 108.1 nm diameter. In addition, an electron beam enhanced particle coalescence is seen in Fig. 10(c) indicating Ostwald ripening.

III. SUMMARY OF EXPERIMENTAL RESULTS AND DISCUSSION

Au thin films deposited by physical vapor deposition technique consist of variously sized particles and clusters, including MTP with decahedron shape or icosahedron shape. Due to the size-dependent melting temperature of Au particles, and irregular variation of melting temperature of Au clusters, the formation of pore on the diffused Au containing membrane under electron beam irradiation requires extreme care. We carried out several experiments to obtain an Au-C binary mixture membrane via various surface treatments

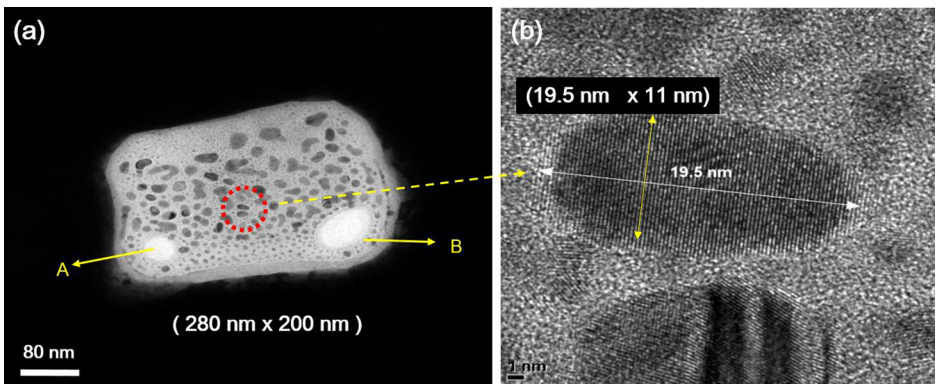

FIG. 8. (Color online) TEM image of the etched area of (~280 × ~200 nm) membrane with Au clusters on the membrane formed by 30 keV Ga ion irradiation for 1 s in (a). An Au cluster (inside the red dotted circle) is magnified to present a (19.5 × 11 nm) size particle.

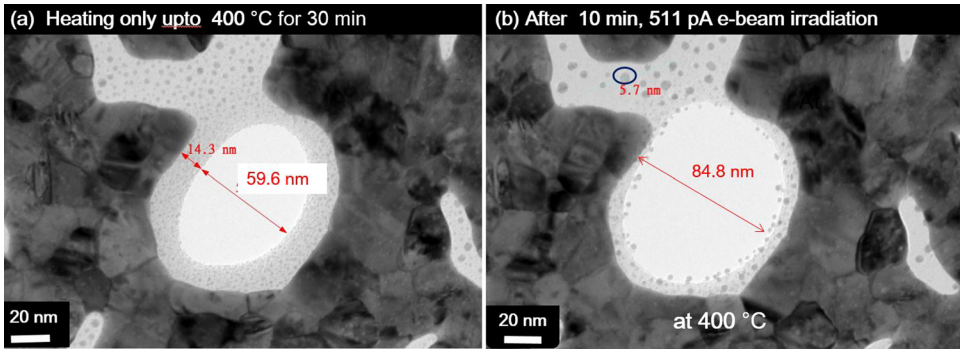

FIG. 9. (Color online) TEM image of a 40 nm thick Au film heated up to 400 °C. A larger hole with a width of 69.6 nm was formed via spinodal dewetting. Numerous tiny Au particles are distributed on the whole gray membrane area in (a). Upon a 300 keV electron beam irradiation for 10 min, coalescing of Au particles via Ostwald ripening are observed. The 59.6 nm diameter hole in (a) became a larger hole increasing its diameter to 84.8 nm in (b). The particle size inside the blue circle is measured to be ~5.7 nm.

including electron beam irradiation by TEM and FESEM, Ga ion beam etching, and thermal heating.

(1) Influence of TEM electron beam on the Au aperture: we found that thermal influence during 300 keV electron beam irradiation is limited to the area where electron beam irradiates. We observed the (13.97×11.70 nm) pore on the diffused membrane only inside the Au aperture where the electron beam irradiated, not on the adjacent Au apertures.
(2) Pore opening and shrinking dependent upon the electron beam current density: For 5 pA electron beam irradiation for 5 min at 300 keV, the Au along with C diffuse into the aperture and the (18×26 nm) size opening forms on the diffused membrane. However, for 10 pA electron beam irradiation for 5 min at 300 keV, the pore membrane evaporated and the (19×39 nm) sized pore became widened to be a (45.7×83.6 nm) size pore. This phenomenon can be attributed to evaporation of carbon and Au atoms from high energy bombardments.
(3) For aperture diameter bigger than the thickness of the Au film, FESEM electron beam irradiation at 2 keV has been used to form the diffused membrane. 1.4 nA electron beam irradiations at 2 keV for 1, 3, 5, and 6 min have been carried out, and the corresponding pore diameters are found to be 145, 78, 46, and 0 nm, respectively. Au clusters were formed on all diffused membranes via Ostwald ripening several months after electron beam irradiations.
(4) An EDS line scan with a 1.5 nm probe diameter and 2.5 nA beam currents has been performed on the electron beam induced membrane. The average atomic concentrations of Au, C and O atoms are found to 80%, ~20%, and less than 10%, from the EDS line scanning analysis. The 207 nm diameter pore on the diffused membrane was also formed under a 2 keV 1.4 nA FESEM electron beam irradiation.
(5) Under 30 keV Ga ion beam etching on a 200 nm thick Au film, the thin (280×200 nm) membrane with many Au clusters was formed. This membrane formed is found to contain the Au and C atoms. The ratio of the average Au atomic concentration to that of C is measured to be 1.14.
(6) Spinodal dewetting and Ostwald ripening during thermal treatments: When the specimen was heated from room temperature to 400 °C, a 40 nm thick Au film became ruptured and holes surrounded with thermally diffused membrane were formed. Under 300 keV electron beam irradiation at 400 °C for 10 min, the hole grew and became bigger with the reduced gray membrane area, and the tiny Au particles distributed on the diffused membrane became larger via Ostwald ripening.

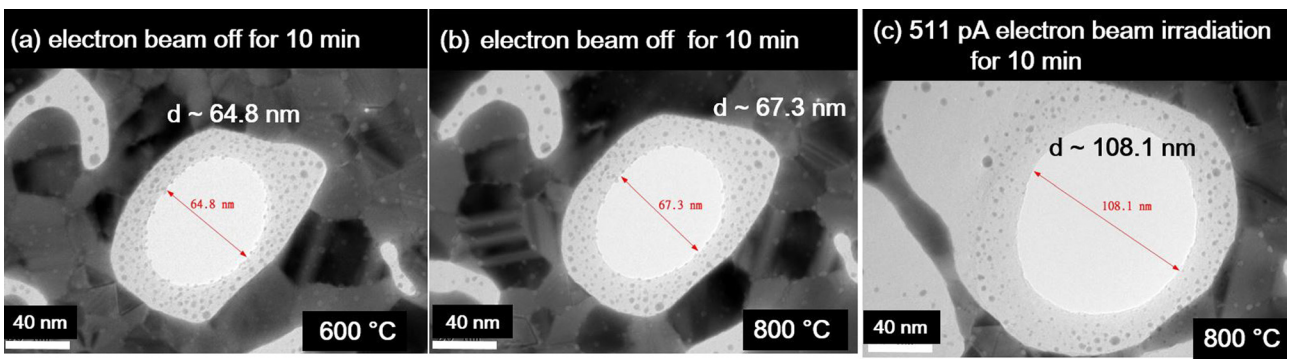

FIG. 10. (Color online) TEM images of a 40 nm thick Au film for 10 min heating at 600 °C in (a) and 800 °C in (b). Upon heating the sample without electron beam irradiation, a pore with 64.8 nm diameter is presented at 600 °C in (a). After a 10 min heating at 800 °C without electron beam irradiation, no significant change is observed; only a slight change from 64.8 to 67.3 nm was observed. However, for a 10 min electron beam irradiation at 800 °C, the pore became bigger and merged into a larger one with its diameter 108.1 nm in (c).

However, without electron beam irradiation, for 10 min heating at 800 and 600 °C, the morphology of the liquid state membrane did present any significant change. For a 300 keV electron beam irradiation at 800 °C for 10 min, the holes on the membrane grew and merged into a larger one with a diameter of 108.1 nm. In addition, an electron beam enhanced particle coalescence is obseved via Ostwald ripening.

Recently, there have been some debates over whether the membrane formed under electron beam irradiations contains Au atoms or not. We have experienced some processing difficulties due to irregular variation of Au melting temperature dependent upon the size and the shape of Au cluster, and to nanoscale local charging of the specimen. However, our experimental results present that the membrane formed under various surface treatments always contains Au atoms and C atoms regardless of the surface treatment types.

IV. CONCLUSION

We have fabricated the nanoscale membrane on the sputter-deposited Au bulk film under various surface treatments. The membranes formed under electron beam irradiations are found to contains Au and C atoms. By controlling the Au concentration and the formation of Au clusters on the membrane, the plasmonic pore can be fabricated with a proper design, and can be utilized as a single molecule optical biosensor.

ACKNOWLEDGMENTS

This work was partially supported by the Basic Science Research Program through National Research Foundation (NRF 2015-R1D1A1A-09056781) and by Global Research Laboratory funding (Nanoplasmonic Integrated Circuits for Ultrafast Information Processing, NRF Grant No. K20815000003-2008-00580).

[1]A. J. Storm, J. H. Chen, X. S.Ling, H. W. Zanbergen, and C. Dekker, Nat. Mater **2**, 537 (2003).
[2]B. McNally, A. Singer, Z. Yu, Y. Sun, Z. Weng, and A. Miller, Nano Lett. **10**, 2237 (2010).
[3]A. S. Prabhu, K. J. Freedman, J. W. F. Robertson, Z. Nikolov, J. J. Kasianowicz, and M. J. Kim, Nanotechnology **22**, 425302 (2011).
[4]H. Chang, S. M. Iqbal, E. A. Stach, A. H. King, N. J. Zaluzec, and R. Bashir, Appl. Phys. Lett. **88**, 103109 (2006).
[5]C. J. Lo, T. Aref, and A. Bezryadin, Nanotechnology **17**, 3264 (2006).
[6]A. S. Mikheyev and M. M. Y. Tin, Mol. Ecol. Resour. **14**, 1097 (2014).
[7]E. C. Hayden, "Nature News," 14 February 2014, http://dx.doi.org/10.1038/nature.2014.14724.
[8]E. C. Hayden, Nature **521**, 15 (2015).
[9]S. S. Choi, M. J. Park, T. Yamaguchi, S. I. Kim, K. J. Park, and N. K. Park, Appl. Surf. Sci. **310**, 196 (2014).
[10]S. S. Choi, M. J. Park, C. H. Han, S. J. Oh, T. Yamaguchi, N. K. Park, J. H. Yoo, K. J. Park, and Y. S. Kim, Surf. Coat. Technol. **306**, 113 (2016).
[11]S. S. Choi *et al.*, Sens. Bio-Sens. Res. **7**, 153 (2016).
[12]S. S. Choi, M. J. Park, C. H. Han, S. J. Oh, S. H. Han, N. K. Park, Y. S. Kim, and H. Choo, J. Vac. Sci. Technol., B **33**, 06F203 (2015).
[13]T. Komoda, J. Phys. Soc. Jpn. **7**, 27 (1968).
[14]D. W. Pashlemy, J. Stowellm, H. Jacob, and T. J. Law, Philos. Mag. **10**, 127 (1964).
[15]S. Ino, J. Phys. Soc. Jpn. **21**, 346 (1966).
[16]M. Schmitt, R. Kusche, B. V. Issendorff, and H. Haberland, Nature **393**, 238 (1998).
[17]Ph. Buffat and J. P. Borel, Phys. Rev. A **13**, 2287 (1976).
[18]H. Li, L. Li, A. Pedersen, Y. Gao, N. Khetrapal, H. Jónsson, and X. C. Zeng, Nano Lett. **15**, 682 (2015).
[19]T. P. Martin, Phys. Rep. **273**, 199 (1996).
[20]K. Kanaya and S. Okayama, J. Phys. D: Appl. Phys. **5**, 43 (1972).
[21]B. T. Wong, M. P. Menguc, and R. R. Balance, J. Heat Transfer **126**, 566 (2004).
[22]H. Sakai, Surf. Sci. **351**, 285 (1996).
[23]M. Lanxner, C. L. Bauer, and R. Scholz, Thin Solid Films **150**, 323 (1987).
[24]G. I. Taylor and D. H. Michael, J. Fluid Mech. **58**, 625 (1973).
[25]A. Howie, Nature **320**, 684 (1986).
[26]E. M. Bringa and R. E. Johnson, Phys. Rev. Lett. **88**, 165501 (2002).
[27]T. Yokota, M. Murayama, and J. M. Howe, Phys. Rev. Lett. **91**, 265504 (2003).
[28]N. Doraiswamy and L. D. Marks, Surf. Sci. **348**, L67 (1996).
[29]P. Williams, Appl. Phys. Lett. **50**, 1760 (1987).
[30]J.-G. Lee and H. Mori, Sci. Technol. Adv. Mater. **5**, 51 (2004).
[31]T. J. Bullough, Philos. Mag. A **75**, 69 (1997).
[32]S. Bysakh, M. Shimojoa, K. Mitsuishi, and K. Furuya, J. Vac. Sci. Technol., B **22**, 2620 (2004).
[33]R. Werner, M. Wanner, G. Schneider, and D. Gerthsen, Phys. Rev. B **72**, 045426 (2005).
[34]B. Westenfelder, J. C. Meyer, J. Biskupek, S. Kurasch, F. Scholz, C. E. Krill III, and U. Kaiser, Nano Lett. **11**, 5123 (2011).
[35]L. D. Marks, Phys. Rev. Lett. **51**, 1000 (1983).
[36]Y. Oshima, Y. Kurui, H. D. Nguen, T. Ono, and K. Takayanagi, Phys. Rev. B **84**, 035401 (2011).
[37]K. Yoshida, A. Bright, and N. Tanaka, J. Electron Microsc. **61**, 99 (2012).
[38]P. W. Voorhees, J. Stat. Phys. **38**, 231 (1985).
[39]M. Kahlweit, Adv. Colloid Interface Sci. **5**, 1 (1975).
[40]J. Zhu, L. Q. Chen, J. Shen, and V. Tikare, Phys. Rev. E **60**, 3564 (1999).
[41]G. Madras and B. J. McCoy, J. Chem. Phys. **119**, 1683 (2003).
[42]J. W. P. Schmelzer, A. S. Abyzov, and J. Möller, J. Chem. Phys. **121**, 6900 (2004).
[43]A. G. Lamorgesea and R. Mauri, Phys. Fluids **17**, 034107 (2005).
[44]J. Bischof, D. Scherer, S. Herminghaus, and P. Leiderer, Phys. Rev. Lett. **77**, 1536 (1996).
[45]S. Herminghaus, K. Jacobs, K. Mecke, J. Bischof, A. Fery, M. Ibn-Elhaj, and S. Schlagowski, Science **282**, 916 (1998).
[46]See supplementary material at http://dx.doi.org/10.1116/1.4994828 for the average atomic concentration data on the membrane area formed during FIB etching.